Talanta 190 (2018) 263–268

Contents lists available at ScienceDirect

Talanta

journal homepage: www.elsevier.com/locate/talanta

A novel biosensor based on Au@Ag core-shell nanoparticles for sensitive detection of methylamphetamine with surface enhanced Raman scattering

Kang Mao[a], Zilei Zhou[a], Sheng Han[a], Xiaodong Zhou[b], Jiming Hu[b], Xiqing Li[a,*], Zhugen Yang[c,*]

[a] Laboratory for Earth Surface Processes, College of Urban and Environmental Sciences, Peking University, Beijing 100871, China
[b] Key Laboratory of Analytical Chemistry for Biology and Medicine (Ministry of Education), College of Chemistry and Molecular Sciences, Wuhan University, Wuhan 430072, China
[c] School of Engineering, University of Glasgow, Oakfield Avenue, Glasgow G12 8LT, United Kingdom

ARTICLE INFO

Keywords:
Methylamphetamine
Au@Ag
Aptamer
SERS, illicit drug of abuse

ABSTRACT

We describe a novel biosensing strategy for sensitive detection of methylamphetamine (MAMP) based on surface enhanced Raman scattering (SERS) by the mediation of spacing between 4-mercaptobenzoic acid (4-MBA) labeled Au@Ag core-shell nanoparticles (Au@Ag). To achieve a favorable SERS substrate, Au@Ag shell-core nanoparticle was synthesized with seeds growth method and well characterized by SEM, TEM and UV–vis spectrometer. The uniform Au@Ag shows an excellent dispersion ability for SERS detection. Under the optimized conditions, the novel biosensor shows a good logarithm linear correlation with the concentration of MAMP ranging from 0.5 ppb to 40 ppb (R^2 = 0.986), with a limit of detection at 0.16 ppb of MAMP (3σ). Furthermore, our biosensors hold an excellent selectivity, demonstrated by the negligible interference from the detection of other illicit drugs and metabolites. The concentrations determined with our biosensor from spiked MAMP in human urine sample fell within the same range with the results from mass spectrometry. This indicates that our sensor has a clear potential for the rapid detection of illicit drug in real samples.

1. Introduction

The abuse of illicit drugs is a worldwide problem that has severe societal consequences, such as loss of lives and health of abusers, increased treatment costs, and higher incidence of crimes [1–4]. Among the abuse of illicit drugs, methylamphetamine (MAMP)/methamphetamine (METH) is the second widely abused illicit drug on the world [5]. To monitor and control abuse of MAMP, a variety of sample matrices such as urine and blood need to be analyzed at the point-of-site. Traditional methods for quantitative detection of MAMP include gas chromatography coupled with mass spectrometry [6], high performance liquid chromatography coupled with mass spectrometry [2,3], ion mobility spectrometry [7], imaging mass spectrometry [8], etc. Although these methods are robost and sensitive, they are mostly laboratory-based, requiring expensive facility and highly-trained personnel for interpretation of data. Therefore, there is a great need of developing simple and rapid assay.

Biosensors have a great potential for rapid detection of illicit drug even in the complex matrixes [9]. Moreover, they do not require tedious sample preparation, complex pretreatment procedures, expensive instruments and professional personnel. The rapid-developing nanotechnology has provided a new opportunity for improving the performance of sensors in terms of sensitivity and selectivity. Mohsen et al. [10,11] firstly developed an electrochemical impedance spectroscopic sensing for methylamphetamine detection using a specific aptamer by SELEX. Shi et al. [5] developed a colorimetric and naked-eye determination of urinary methylamphetamine based on aptamers and the salt-induced aggregation of unmodified gold nanoparticles. Yarbakht and co-workers [12] described an unmodified gold nanoparticles as a colorimetric probe for visual detection of methylamphetamine. Our research group also proposed a novel colorimetric biosensor based on non-aggregated Au@Ag core-shell nanoparticles for methylamphetamine with an promising limit of detection (LOD) at 0.1 nM and a broad dynamic range spanning from 0.5 to 200 nM [13]. However, the aptamer-based sensors involves immobilization of DNA probes onto nanoparticles, and the potential folding of DNA aptamers may limit the sensitivity and specificity.

Surface-enhanced Raman scattering (SERS) technique holds great potential for the detection at the point-of-need, because there are commercially-available portable device for filed- testing. SERS is an extremely sensitive analytical technique mainly based on the giant electromagnetic enhancement induced by localized plasmon resonance

* Corresponding authors.
E-mail addresses: xli@urban.pku.edu.cn (X. Li), zhugen.yang@glasgow.ac.uk, zhugen.yang@gmail.com (Z. Yang).

https://doi.org/10.1016/j.talanta.2018.07.071
Received 22 March 2018; Received in revised form 17 July 2018; Accepted 22 July 2018
Available online 25 July 2018

(LPR) of nanoscale noble metal surfaces [14,15]. SERS has been widely used to biomedical and environmental analysis of molecule, pathogen, cell and even the whole living animal [15]. Apart from its high sensitivity, SERS also possesses other inherent advantages, such as a wide range of excitation wavelengths, low photo-bleaching and high-resolution spectroscopic bands. Recently, the gold nanoparticles-based SERS sensor has attracted increasing attention for the rapid detection of DNA [16], heavy metal ions [17] and proteins [18]. To improve the sensitivity of SERS assay, novel structures of AuNPs have been synthesized [19–21]. For example, Yan et al [20] designed a Au@Ag core-shell nanostructures with embedding Cy5-labeled DNA aptamer to target chloramphenicol using SERS for detection, which is able to selectively detect as low as 0.19 pg mL^{-1} chloramphenicol.

In this paper, we present an approach to effectively synthesize Au@Ag core-shell nanopartics for the SERS detection of MAMP. The SERS effect of Au@Ag and AuNPs was compared and the concentration of 4-MBA was optimized to allow the biosensor for the detection as low as 0.16 ppb MAMP, spanning a logarithm concentration range from 0.5 ppb to 40 ppb, with a promising selectivity. The evaluation of MAMP spiked in urine sample demonstrated that the matrix effect is very tiny and the results were comparable with mass spectrometry data. The results showed our sensor has a clear potential for the detection of real sample.

2. Experiment

2.1. Reagents

Oligos (5′-ACGGTTGCAAGTGGGACTCTGGTAGGCTGGGTAATT TGG-3′) was purchased from Sangon Biotech (Shanghai, China) Co., Ltd. and purified by HPLC. Trisodium citrate (99.8%) was obtained from Sigma-Aldrich (USA). $HAuCl_4{\cdot}3H_2O$ (99.9%) and $AgNO_3$ (99.9%) were purchased from Shanghai Chemical Reagent Co., Ltd. (Shanghai, China). 4-MBA (99.9%) was provided by Heowns Biochemical Technologies Co., Ltd. (Tianjin, China). All illicit drugs and metabolites were the standard substances dissolving in methanol with the concentration of 10 ppm, purchased from Cerilliant (Round Rock, TX, USA). Urines were collected from the volunteer in our laboratory. Urine sample collection and experiments were carried out in accordance with a protocol approved by the ethics committee of Peking University and with informed consent of the volunteer. 0.22 μm membrane filters were purchased from ANPEL Laboratory Technologies (Shanghai, China) Inc. Ultrapure water with an electrical resistance larger than 18.2 MΩ was used throughout the experiment. To mimic the physiological condition, phosphate buffer saline (PBS) was used as the buffer. All solutions and the buffers in the experiments were prepared using ultrapure water. All glasswares were cleaned with aqua regia (volume ratio HCl/HNO_3 = 3:1) and rinsed with ultrapure water throughout the experiment.

2.2. Apparatus

UV spectra of Au NPs and Au@Ag were obtained using a 500 μL quartz cell with a path length of 1 cm by UV–vis spectrometer (Perk Elmer, USA). The morphology of Au@Ag was characterized by scanning electron microscope (SEM). Transmission Electron Microscope images of Au@Ag were obtained using a JEM-2100 (HR) microscope at an acceleration voltage of 200 kV. SERS spectra was collected according to the previous protocol with some modification as following [22]. SERS spectra were obtained using a confocal microscope (Renishaw Invia Raman spectrometer, Invia, U.K.). He-Ne laser with 532 nm radiations was used for excitation. A 50 mm long working distance lens (Olympus) collected the scattering light to the charge-coupled device (CCD) detector. The collecting parameters of each SERS spectrum were exposed for 10 s and integrating 3 times over a spectral. The Raman spectrometer was calibrated by a silicon wafer at 520 cm^{-1} Raman shift before SERS measurement. The HPLC-MS/MS used a UFLCXR-LC system (Shimadzu, Japan) with a Phenomenex Gemini C18 column (100 mm × 2 mm, 3 μm) and an ABI 4000 triple quadrupole mass spectrometer (AB SCIEX, USA). The pH measurements were carried out on a model UB-7 digital ion analyzer (Denver Instrument, America).

2.3. Synthesis of 4-MBA modification Au@Ag core-shell nanoparticles

Au@Ag was synthesized by referring to the methods reported in previous literatures with slightly modification [23]. In brief, gold nanoparticles with a diameter of 30 nm were prepared by reduction of gold (III) chloride hydrate using trisodium citrate. Specifically, 50 mL 0.01% (w/w) $HAuCl_4$ was reduced by 750 μL 1% (w/w) trisodium citrate solution at 100 °C under vigorous magnetic stirring for 15–20 min until the solution turned from colorless to light red. The prepared red-colored Au particles were used as seed particles. Then 600 μL of $AgNO_3$ solution (0.5%, w/w) was added to 100 mL of boiling gold seed solution. Afterwards, 1 mL of sodium citrate solution (1%, w/w) was used as the reducing agent and added dropwise with stirring. The solution was boiled for 1 h. The Au@Ag core-shell nanoparticles were cooled down to room temperature. 1 mM 4-MBA solution dissolved in ethanol was added to Au@Ag for a final concentration from 1 μM to 10 μM. The solution was kept standing for 2 h at room temperature, followed by centrifugation at 4500 rpm for 15 min for three times to remove the excess of unbound 4-MBA. At last, the oily 4-MBA modified Au@Ag in the bottom was re-dispersed in phosphate buffer (1 mM, pH 7.0).

2.4. Measurement procedures

The SERS measurements were carried out in the absence or presence of MAMP by using a Raman spectrometer. Briefly, MAMP aptamer was dissolved in PBS (10 mM, pH 7.2). MAMP standards at various concentrations were prepared by diluting MAMP in PBS buffer (10 mM, pH 7.2). A total volume of 100 μL of reaction mixture containing aptamer (100 nM) and MAMP (0–800 ppb) was incubated at room temperature for a designed time. Then, the reaction mixture was added to the buffer solution of Au@Ag (900 μL) for SERS measurements.

To compare the specificity of the method for MAMP, other illicit drugs and metabolites were measured at the same condition. 100 μL of reaction mixture containing MAMP and ketamine, norketamine, morphine, methadone, cocaine, mephedrone, and cathinone were separately incubated at room temperature for 30 min. Then, the reaction mixture was added to Au@Ag for SERS measurements.

To evaluate the feasibility of our sensors for complex matrix detection, diluted urine sample was tested. We collected the urine samples from a volunteer. The 100-fold diluted human urine containing spiked MAMP (0, 0.5, 5, and 50 ppb) was analyzed with the same procedure by SERS. The measured concentrations were compared with those determined using high performance liquid chromatography-tandem mass spectrometer (HPLC-MS/MS). However, the measurement with our sensors does not need well-trained personnel, which also holds a fast-response time and potential for use in low-setting areas.

3. Results and discussion

3.1. Characterization of AuNPs and Au@Ag

As shown in Fig. 1, the UV–vis spectra of the original Au NPs, and Au@Ag. Au NPs exhibit an absorbance band at 520 nm. A significant red-to-yellow color change between AuNPs and Au@Ag can be easily visualized by the naked eyes (Fig. 1b). The presence of new bands at 510 nm and 400 nm indicates the formation of the Ag shell. This is because AuNPs and Au@Ag have different frequencies of surface plasmon resonance (SPR) in spite of the same particle size. Fig. 1a showed that the average diameter of Au@Ag core-shell nanoparticle was approximately 40 nm. However, the contrast of the shell-silver nano particles is different from that of the core-AuNP in HR-TEM image

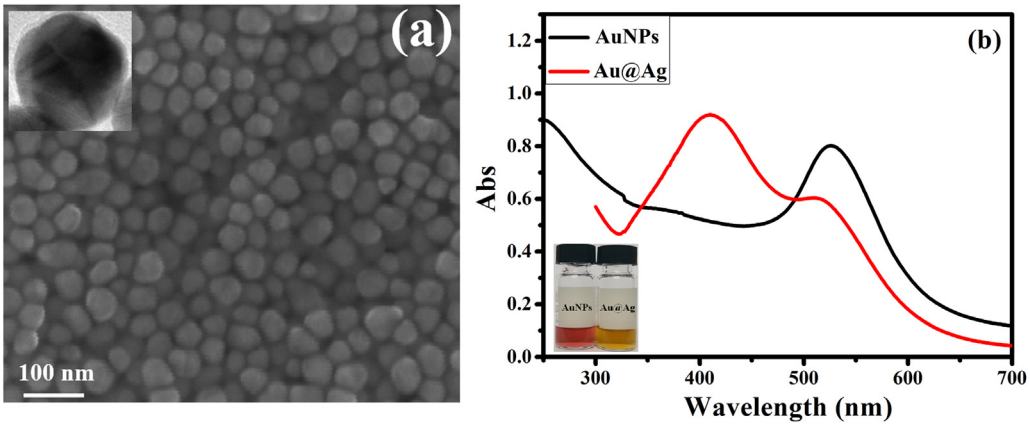

Fig. 1. Scanning electron microscope (SEM) image of as-prepared Au@Ag core-shell nanoparticles (the inset shows the TEM image of single Au@Ag particle) (a) and UV–vis spectra of Au@Ag and AuNPs (the inset shows the color of AuNPS (red) and Au@Ag (yellow)) (b).

(the inset of Fig. 1a). The data demonstrate that the designed nano particles were successfully synthesized, enabling the SERS detection of MAMP.

3.2. Sensing principle

A biosensor is a small device with a biological receptor that generates a signal (electrochemical, optical, nanomechanical, mass sensitive, etc.) in the presence of an analyte {Yang, 2015 #281} [Environ Sci Technol 49(10): 5845-5846]. In our sensor, the biological receptor is DNA aptamer and the detection signal is Raman signal of 4-MBA enhanced by Au@Ag. The aptamer is a sequence of oligonucleotides with high binding affinity and specificity to target utilizing the systematic evolution of ligands by exponential enrichment (SELEX) technology.

This SERS strategy combined MAMP aptamer with Raman labeled Au@Ag core-shell nanoparticles, which greatly enhanced the performance of SERS. 4-MBA and MAMP aptamer were absorbed on Au@Ag to serve as a SERS donor. Scheme 1 shows the design of the assay for MAMP. 4-MBA was modified onto Au@Ag via Au-S bonds, serving as a Raman reporter molecule that provided a simple and narrow characteristic peak. The MAMP added into homogeneous Raman labeled Au@Ag specifically bound to MAMP aptamer, making the aptamer displace from the surface of Au@Ag and subsequently leading to aggregation of Au@Ag. As a consequence, the signal of Raman reporter molecule 4-MBA was enhanced due to the formation of SERS “hot spots”. The addition of different concentrations of MAMP could result in the corresponding amount of MAMP aptamer displacement from the surface of Au@Ag, and corresponding aggregation degree of Au@Ag. Therefore, the signal intensity of 4-MBA is proportional to the concentrations of MAMP, which enables us to construct a novel and simple MAMP biosensor.

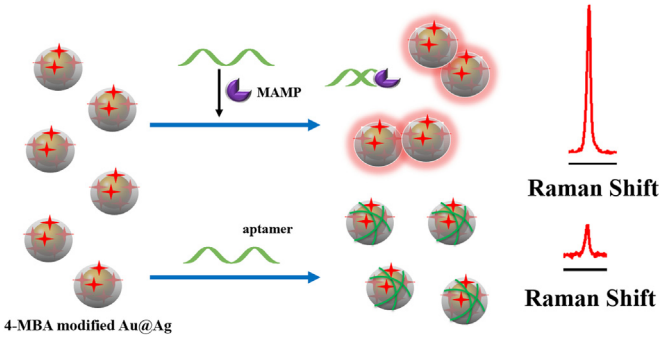

Scheme 1. Schematic representation of SERS detection of MAMP based on Au@Ag core-shell nanoparticles.

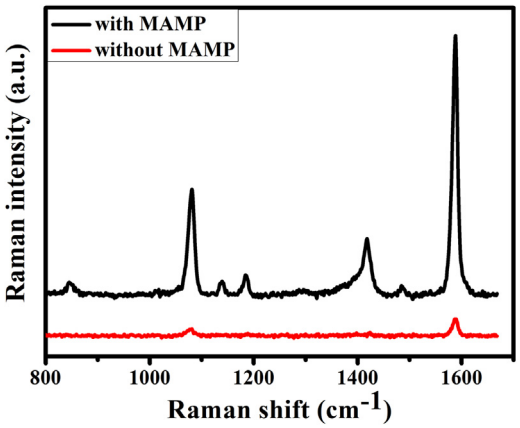

Fig. 2. The Raman spectra of 4-MBA (5 μM) in the absence of MAMP (red curve) and the change of Raman spectra intensity in the presence of MAMP (black curve) (10 ppb) due to aggregation of Au@Ag core-shell nanoparticles. All these Raman spectra were recorded in PBS buffer at room temperature.

We firstly test the feasibility of this strategy to detect MAMP. In the control experiment, when MAMP aptamer was added without MAMP, the SERS signal has no significant Raman enhancement (Fig. 2, red curve), indicating that MAMP aptamer alone had no interference to this analytical platform. This is because MAMP aptamer was effectively absorbed on Au@Ag by means of coordination interaction between N atom of base and Au@Ag, which has a protection for Au@Ag. When MAMP was introduced, the SERS intensity increased dramatically (Fig. 2, black curve), due to the formation of the MAMP-aptamer complex. In other words, there is a competition between MAMP and 4-MBA labeled Au@Ag to bind with the MAMP aptamer. The addition of MAMP into homogeneous Raman labeled Au@Ag could specifically bind with the MAMP aptamer, making the aptamer displace from the surface of Au@Ag, breaking the overall charge balance on the surface of Au@Ag, and ultimately leading to aggregation of Au@Ag. As a consequence, the signal intensity of Raman reporter molecule 4-MBA was significantly enhanced due to the aggregation of Au@Ag and the formation of SERS “hot spots”, which allow for the sensitive detection of MAMP.

3.3. Optimization of the detection conditions

In order to evaluate the superior SERS effect of Au@Ag, we compared the SERS signals from AuNPs and Au@Ag with the same particle diameter. According to Fig. 3a, the Raman intensity of 4-MBA absorbed on Au@Ag was much higher than that of 4-MBA on AuNPs. Previous

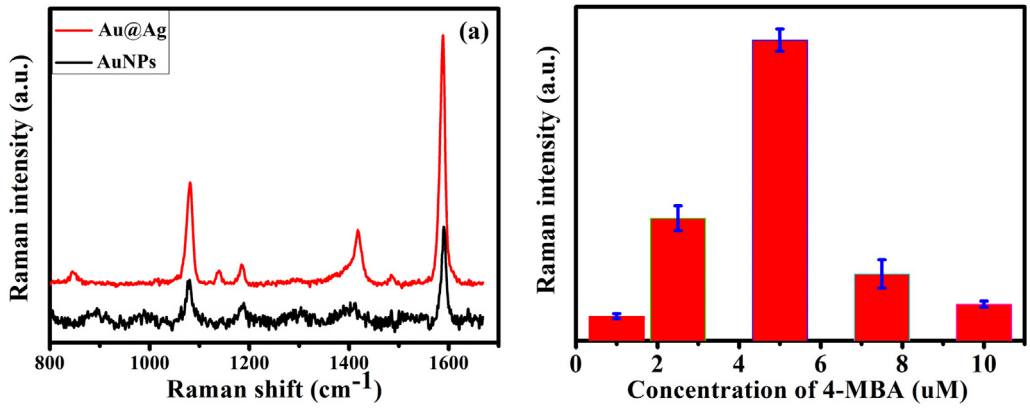

Fig. 3. (a) The Raman spectra of 4-MBA (5 μM) absorbed on the surface of AuNPs and Au@Ag. (b) Optimization of the concentrations of 4-MBA (1, 2.5, 5, 7.5 and 10 μM, respectively.). Error bars represent six replicate measurements (the same for below).

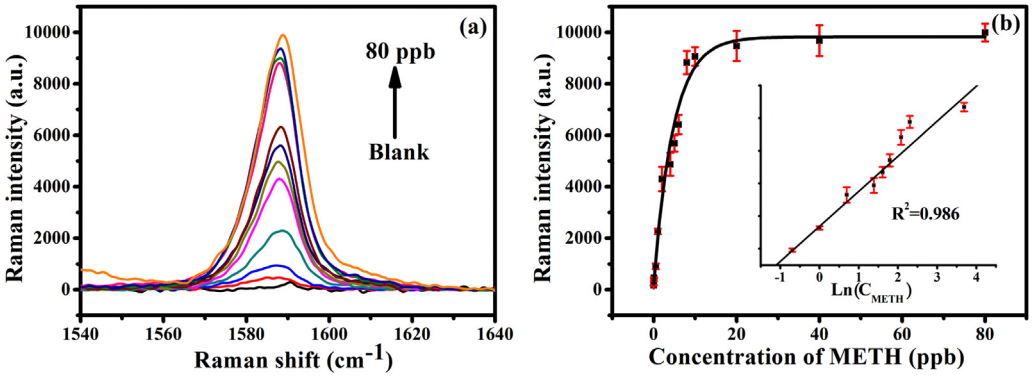

Fig. 4. (a) SERS spectra of 4-MBA added with different concentrations of MAMP in the presence of 10 nM aptamer, with concentrations of MAMP ranging from 0 to 80 ppb from bottom to top. (b) The Raman intensity of 4-MBA at 1588 cm^{-1} varies with different concentrations of MAMP under optimized conditions. The inset shows the linear plot of the constant logarithm of Raman intensity at 1588 cm^{-1} under different concentrations of MAMP in PBS buffer.

literatures reported that Ag nanoparticles produce better SERS effect than that from gold nanoparticles [6]. However, compered to silver NPs, gold NPs are better dispersed with uniform particle size. Furthermore, it was reported that the Au@Ag can obtain the similar high Raman enhancement to that of large Ag nanoparticles (AgNPs) which exhibit stronger Raman enhancement than other metal nanoparticles, and the Au@Ag can also be synthesized to have uniform size and shape using Au NPs as seeds, which is difficult to be obtained for Ag NPs [24,25]. We tried to synthesize the Ag nanoparticles following the protocol, but the particle size and shape are not uniform as showed in Fig. S1. Considering the advantages and disadvantages of such two kinds of nano materials, we successfully synthesized Au@Ag core-shell nanoparticles as SERS substrate and applied it to the MAMP detection system.

We also studied the effects of different concentrations of MBA on Raman signal enhancement. Fig. 3b shows that Raman intensity of 4-MBA changed dramatically as the concentration of MBA increased from 1 to 10 μM. According to previous reports [5], this is because too low concentration of 4-MBA couldn't be sufficient absorbed on the surface of Au@Ag, resulting in low Raman intensity of 4-MBA, while extremely high concentration of 4-MBA may destroy the stability of the dispersed Au@Ag solution, causing aggregation of Au@Ag and low Raman intensity. We optimized the concentrations of 4-MBA to be 5 μM.

3.4. Evaluation of the analytical performance

Under the optimized conditions, the sensitive quantification of MAMP was achieved by monitoring the SERS peaks of 4-MBA labeled on Au@Ag on different spots of three independent samples at various concentrations. Fig. 4a presents the SERS spectra of 4-MBA modified Au@Ag upon the addition of aptamer incubated with different amountconcentratons of MAMP for 30 min. It was suggested that the Raman intensity of peak at 1588 cm^{-1} drastically increased with the increasing concentration of MAMP from 0 to 80 ppb owing to the increase of "hot spots" region and the fact that more MAMP introduced, more MAMP-aptamer complex were formed. Furthermore, the position of characteristic peak of 4-MBA at 1588 cm^{-1} did not change with the increasing MAMP concentration, indicating the specific correspondence with MAMP.

Fig. 4b shows the SERS intensity at 1588 cm^{-1} varies with the concentration of MAMP from 0 to 80 ppb, which has a nearly exponential increasing curve within the tested concentration. To clearly demonstrate the detection for MAMP, six replicates of SERS spectra from 4-MBA were recorded at each concentration from 0 to 80 ppb. The inset of Fig. 4b shows a good linear relationship between the natural logarithm over concentration of MAMP ranging from 0.5 ppb to 40 ppb. The regression equation is $y = 2365.7 + 2146.3x$ (where x is logarithm of the MAMP concentration in ppb level, y is the SERS intensity of peak at 1588 cm^{-1}) with a squared correlation coefficient of 0.986. The lLOD of the SERS sensor for MAMP was determined to be 0.16 ppb according to the 3 times standard deviation rule. This value is much lower than 1000 ng mL^{-1}, the threshold of positive methylamphetamine detection in urine samples recommended by the National Institute on Drug Abuse of United States. Furthermore, compared with other methods using aptamer as the probe, our biosensor has a comparable sensitivity (Table 1).

To evaluate the specificity of the method, our sensors are used to detect other illicit drugs and metabolites including ketamine, norketamine, morphine, methadone, cocaine, mephedrone, and cathinone (500 ppb) (Fig. 5a). After incubation of aptamer with these targets, the mixture was added to 4-MBA modified Au@Ag. Fig. 5a shows that the SERS intensity of 4-MBA at 1588 cm^{-1} did not decrease significantly. Furthermore, the SERS signals obtained from ketamine, norketamine, morphine, methadone, cocaine, mephedrone, and cathinone were

Table 1
The MAMP detection comparison of our assay with other approaches.

Method construct	Read out	Analytical ranges	LOD	Ref.
DNA-AuNPs	Electrochemical impedance spectroscopy	–	nM level	[10]
DNA-AuNPs	Colorimetric and bare eye	2–10 μM	0.82 μM	[5]
DNA-AuNPs	Colorimetric and bare eye	5–400 μM	–	[12]
DNA -Au@Ag	Colorimetric and bare eye	0.5–200 nM	0.1 nM	[13]
DNAenzyme	Colorimetric and bare eye	8–500 nM	0.5 nM	[26]
Boron-doped diamond electrode	Electrochemical analysis	0.07–80 μM	50 nM	[27]
DNA-Au@Ag	SERS	0.5–40 ppb (3.4–268.0 nM)	0.16 ppb (1.1 nM)	This study

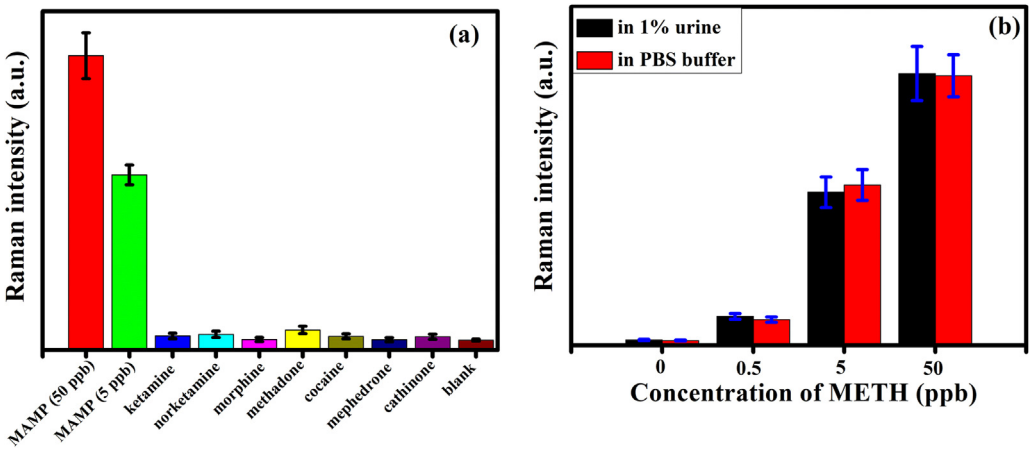

Fig. 5. (a) Evaluation of the specificity of the SERS biosensor. Variation of SERS intensity of 4-MBA modified Au@Ag at 1588 cm^{-1} after separate incubation of aptamer (10 nM) with MAMP (5 and 50 ppb), ketamine (500 ppb), norketamine (500 ppb), morphine (500 ppb), methadone (500 ppb), cocaine (500 ppb), mephedrone (500 ppb), and cathinone (500 ppb) and (b) recovery test of MAMP spiked in 1% human urine compared with PBS buffer.

rather lower than that from the MAMP. It is likely due to the non-specific adsorption of aptamer on the surface of Au@Ag, which may prevent the aggregation. However, when MAMP and the aptamer was incubated under the same condition, followed by the addition to 4-MBA modified Au@Ag, SERS intensity of 4-MBA at 1588 cm^{-1} increased significantly, indicating that the substrate has a good specificity toward MAMP. The addition of interferences even at a much higher concentration than MAMP may only induce a negligible SERS response, indicating that the proposed sensors holds a promising selectivity for the MAMP assay.

3.5. Detection of MAMP in urine sample

We spiked MAMP into human urine for evaluation of the ability of our sensors for real sample detection. The human urine samples were firstly filtered with 0.22 μm membrane filters and diluted to 100 times with PBS buffer to minimize the effects of inhibitors. Various concentration (0, 0.5, 5, and 50 ppb) of standard MAMP were spiked into urine and measured under the same condition. Fig. 5b shows that the SERS response from the samples spiked in urine are similar with those in PBS buffer and we can achieve a recovery at around 91–102%, indicating that the matrix effect is very tiny. The MAMP concentrations measured using HPLC-MS/MS (Fig. S2, red bar) ranging from 0.5 to 50 ppb. MAMP concentrations (Fig. S2, black bar) detected with our biosensor fell within the same range (RSD = 1.2%, n = 6), were almost the same with those from HPLC-MS/MS, indicating that our sensors have a clear potential for the detection of MAMP in real biological samples.

4. Conclusion

In summary, a novel biosensor based on SERS enhanced with Au@Ag core-shell nanoparticles and DNA aptamer was developed for the sensitive and selective detection of MAMP. To achieve a favorable SERS substrate, Au@Ag shell-core nanoparticle was synthesized with seeds growth method, which showed an excellent dispersion ability for SERS detection. The synthesized Au@Ag nano materials were well characterized with TEM and UV–vis spectrometry. The proposed MAMP sensors is able to detect as low as 0.16 ppb, with a broad dynamic range from 0.5 ppb to 40 ppb. Furthermore, the biosensor also holds a high selectivity, demonstrated by the negligible interference from the detection of other illicit drugs and metabolites. METH concentrations analyzed using our biosensor fell within the same range by the detection of spiked MAMP in human urine sample, and the results are in agreement with those determined by HPLC-MS/MS, demonstrating a great potential for the detection of real urine samples. More importantly, this highly sensitive and selective sensor could serve as a generic platform for the detection of a range of illicit drugs and metabolites by replacing the respective DNA aptamer. This platform will potentially serve as a rapid tool for screening of illicit drug of abuse, as well as environment monitoring and biomedical diagnosis.

Acknowledgement

We gratefully acknowledge the support from the Natural Science Foundation of China (NSFC) (No. 41371442 and 41401566). ZY thanks UK NERC personal fellowship grant (NE/R013349/1).

Appendix A. Supplementary material

Supplementary data associated with this article can be found in the online version at doi:10.1016/j.talanta.2018.07.071.

References

[1] S. Galanie, K. Thodey, I.J. Trenchard, M.F. Interrante, C.D. Smolke, Complete biosynthesis of opioids in yeast, Science 349 (2015) 1095–1100.
[2] P. Du, K. Li, J. Li, Z. Xu, X. Fu, J. Yang, H. Zhang, X. Li, Methamphetamine and ketamine use in major Chinese cities, a nationwide reconnaissance through sewage-based epidemiology, Water Res. 84 (2015) 76–84.
[3] B. Subedi, K. Kannan, Mass loading and removal of select illicit drugs in two wastewater treatment plants in New York State and estimation of illicit drug usage in communities through wastewater analysis, Environ. Sci. Technol. 48 (12) (2014) 6661–6670.
[4] United Nations Office on Drugs and Crime, World Drug Report 2015, 2015.

[5] Q. Shi, Y. Shi, Y. Pan, Z. Yue, H. Zhang, C. Yi, Colorimetric and bare eye determination of urinary methylamphetamine based on the use of aptamers and the salt-induced aggregation of unmodified gold nanoparticles, Microchim. Acta 182 (3) (2015) 505–511.
[6] K. Okajima, A. Namera, M. Yashiki, I. Tsukue, T. Kojima, Highly sensitive analysis of methamphetamine and amphetamine in human whole blood using headspace solid-phase microextraction and gas chromatography–mass spectrometry, Forensic Sci. Int. 116 (1) (2001) 15–22.
[7] M.L. Ochoa, P.B. Harrington, A. Chem, Detection of methamphetamine in the presence of nicotine using in situ chemical derivatization and ion mobility spectrometry, Anal. Chem. 76 (4) (2004) 985–991.
[8] S. Muramoto, T.P. Forbes, A.C.V. Asten, G. Gillen, A novel test sample for the spatially resolved quantification of illicit drugs on fingerprints using imaging mass spectrometry, Anal. Chem. 87 (2015) 5444–5450.
[9] Z. Yang, E. Castrignanò, P. Estrela, C.G. Frost, B. Kasprzykhordern, Community sewage sensors towards evaluation of drug use trends: detection of cocaine in wastewater with DNA-directed immobilization aptamer sensors, Sci. Rep. 6 (2016) 21024–21034.
[10] M. Ebrahimi, M. Johariahar, H. Hamzeiy, J. Barar, O. Mashinchian, Y. Omidi, Electrochemical impedance spectroscopic sensing of methamphetamine by a specific aptamer, Bioimpacts 2 (2) (2012) 91–95.
[11] M. Ebrahimi, H. Hamzeiy, J. Barar, A. Barzegari, Y. Omidi, Systematic evolution of ligands by exponential enrichment selection of specific aptamer for sensing of methamphetamine, Sens. Lett. 11 (3) (2013) 566–570.
[12] M. Yarbakht, M. Nikkhah, Unmodified gold nanoparticles as a colorimetric probe for visual methamphetamine detection, J. Exp. Nanosci. 11 (2015) 1–9.
[13] K. Mao, Z. Yang, J. Li, X. Zhou, X. Li, J. Hu, A novel colorimetric biosensor based on non-aggregated Au@Ag core–shell nanoparticles for methamphetamine and cocaine detection, Talanta 175 (2017) 338–346.
[14] M. Moskovits, Surface-enhanced spectroscopy, Rev. Mod. Phys. 57 (3) (1985) 783–826.
[15] J. Kneipp, H. Kneipp, K. Kneipp, SERS-a single-molecule and nanoscale tool for bioanalytics, Chem. Soc. Rev. 37 (5) (2008) 1052–1060.
[16] J. Su, D. Wang, L. Nörbel, J. Shen, Z. Zhao, Y. Dou, T. Peng, J. Shi, S. Mathur, C. Fan, Multicolor gold-silver nano-mushrooms as ready-to-use SERS probes for ultrasensitive and multiplex DNA/miRNA detection, Anal. Chem. 89 (4) (2017) 2531–2538.
[17] L. Song, K. Mao, X. Zhou, J. Hu, A novel biosensor based on Au@Ag core–shell nanoparticles for SERS detection of arsenic (III), Talanta 146 (2016) 285–290.
[18] N. Feliu, M. Hassan, R.E. Garcia, D. Cui, W.J. Parak, R.A. Alvarezpuebla, SERS quantification and characterization of proteins and other biomolecules, Langmuir 33 (2017) 9711–9730.
[19] W. Yan, L. Yang, H. Zhuang, H. Wu, J. Zhang, Engineered "hot" core–shell nanostructures for patterned detection of chloramphenicol, Biosens. Bioelectron. 78 (2016) 67–72.
[20] J. Hao, B. Xiong, X.D. Cheng, Y. He, E.S. Yeung, A. Chem, High-throughput sulfide sensing with colorimetric analysis of single Au-Ag core-shell nanoparticles, Anal. Chem. 86 (10) (2014) 4663–4667.
[21] T. Li, Y. Li, Y. Zhang, C. Dong, Z. Shen, A. Wu, A colorimetric nitrite detection system with excellent selectivity and high sensitivity based on Ag@Au nanoparticles, Analyst 140 (4) (2015) 1076–1081.
[22] W. Fang, X. Zhang, Y. Chen, L. Wan, W. Huang, A. Shen, J. Hu, Portable SERS-enabled micropipettes for microarea sampling and reliably quantitative detection of surface organic residues, Anal. Chem. 87 (18) (2015) 9217–9224.
[23] A. Shen, L. Chen, W. Xie, J. Hu, A. Zeng, R. Richards, J. Hu, Triplex Au-Ag-C core-shell nanoparticles as a novel Raman label, Adv. Funct. Mater. 20 (6) (2010) 969–975.
[24] B. Liu, G. Han, Z. Zhang, R. Liu, C. Jiang, S. Wang, M.-Y. Han, Shell thickness-dependent raman enhancement for rapid identification and detection of pesticide residues at fruit peels, Anal. Chem. 84 (1) (2012) 255–261.
[25] J.F. Li, Y.J. Zhang, S.Y. Ding, R. Panneerselvam, Z.Q. Tian, Core–shell nanoparticle-enhanced raman spectroscopy, Chem. Rev. 117 (7) (2017) 5002–5069.
[26] K. Mao, Z. Yang, P. Du, Z. Xu, Z. Wang, X. Li, G-quadruplex–hemin DNAzyme molecular beacon probe for the detection of methamphetamine, RSC Adv. 6 (67) (2016) 62754–62759.
[27] L. Švorc, M. Vojs, P. Michniak, M. Marton, M. Rievaj, D. Bustin, Electrochemical behavior of methamphetamine and its voltammetric determination in biological samples using self-assembled boron-doped diamond electrode, J. Electroanal. Chem. 717–718 (2) (2014) 34–40.